

Evaluation of eggshell lime as green accelerator on palm oil fuel ash concrete production: Effect of thermal treatment

Nur Hafizah A. Khalid^{a,b,*}, Nur Nadhira A. Rasid^a, Abdul Rahman Mohd.Sam^b,
Zaiton Abdul Majid^c, Norazah Basar^c, Muhammad Akbar Caronge^d, Ghasan Fahim Huseien^{e,**}

^a Faculty of Civil Engineering, Universiti Teknologi Malaysia, 81310 Johor Bahru, Johor, Malaysia

^b UTM Construction Research Centre, Institute for Smart Infrastructure and Innovative Construction, School of Civil Engineering, Faculty of Engineering, Universiti Teknologi Malaysia, 81310 Johor Bahru, Johor, Malaysia

^c Department of Chemistry, Faculty of Science, Universiti Teknologi Malaysia, UTM, 81310 Johor Bahru, Johor, Malaysia

^d Department of Civil Engineering, Faculty of Engineering, Universitas Hasanuddin, Makassar 92171, Indonesia

^e Institute of Architecture and Construction, South Ural State University, Lenin Prospect 76, 454080 Chelya-binsk, Russia

ARTICLE INFO

Keywords:

Eggshell powder
Calcined eggshell
Palm oil fuel ash
Accelerator
SiO₂-CaO reactivity

ABSTRACT

This paper presents the potential use of eggshell powder (ESP) as green accelerator in ground palm oil fuel ash (GPOFA) concrete. Three categories of ESPs namely uncarbonised ESP (UC-ESP), carbonised ESP (C-ESP) and decarbonised ESP (DC-ESP) corresponding to no calcination and calcination at temperatures of 750 and 1000 °C, respectively, were prepared and studied. In addition, ESPs were used as cement replacement (0, 5, 10, 15, and 20 wt%) in GPOFA concrete and their performance were examined in term of reactivity, workability, heat hydration, compressive strength and microstructure performance. It was found that the presence of UC-ESP, C-ESP and DC-ESP can provide a low, medium and superior accelerator behaviour in the early age of GPOFA concrete. Overall, the GPOFA concrete combined with DC-ESP revealed an excellence SiO₂-CaO reactivity, giving a twice compressive strength at early age and provides inductive hydration behaviour with low hydration temperature and significant improvement in dense gels formulation. Hence, this study provides a positive impact for rapid construction technology. As a conclusion, modified ESP is a highly potential as partial cement replacement and accelerator for concrete.

1. Introduction

In the recent development of the construction industry, some applications require the rapid achievement of early strength such as precast concrete. There are two major stages of strength development namely, at the early stage and later stage. These strengths development is governed by different types of the accelerator and pozzolanic materials used in the mix [1,2]. One of the methods to attain such early strength is through the incorporation of accelerators in concrete. The accelerators for concrete early strength development could be enhanced by alites which contains calcium-based materials. As such, most of the accelerators applied in concrete development nowadays are chemically based and might not be environmental-friendly. Materials with high amount of calcium oxide (CaO) highly recommended as cement' accelerator agent to improve the hydration process, formulate extra calcium

hydroxide, shorten the setting time and increase the rate of early strength development of product concrete [3,4].

Limestone is derived from inorganic calcium based minerals and is the most versatile chemicals to the real-life applications [1]. Quicklime and hydrated lime are the most two limestone use in most industry applications. The most usage of lime is known to be used for cement and concrete production [2] and some others civil engineering application [3–8]. Apart from natural lime, bio-lime derived from chicken eggshell can be regarded as green and renewable lime with comparable properties to that of natural lime. This bio-lime has been widely used in fertilizer, soil stabilizer, health supplements [9], cosmetic improvements [10], wastewater treatment by removing heavy metal component [8,10,11] and catalyst for bio-diesel [7,12]. Globally, about 250,000 tonne of eggshell waste produced annually [13]. In Malaysia alone, approximately 58 million eggshells were produced [14] and need to be disposal

* Corresponding author at: Faculty of Civil Engineering, Universiti Teknologi Malaysia, 81310 Johor Bahru, Johor, Malaysia.

** Corresponding author.

E-mail addresses: nur_hafizah@utm.my (N.H.A. Khalid), eng.gassan@yahoo.com (G.F. Huseien).

off.

Consequently, it is highly recommended to produce cementitious replacement materials from the agro-waste as mentioned earlier which could contribute to both the early and later strength of concrete. One of the alternatives to solve this problem is by selecting green materials that could help in boosting the early age strength of concrete (acting as a catalyst), such as bio-lime inspired eggshell that is rich in CaO and the enhancement in later concrete strength with materials that are rich in SiO₂ such as GPOFA. Eggshell is rich (90 wt%) in calcium carbonate (CaCO₃) but demonstrating a very low cementitious reactivity [15]. However, transforming calcium carbonate (CaCO₃) to calcium oxide (CaO) using calcination process could potentially enhance its reactivity with pozzolans (SiO₂) in cement concrete [12,15–17]. Theoretically, the ideal temperature for the transformation of CaCO₃ into CaO is about 800 °C or higher [12]. Once the calcination temperature exceeded 900 °C more porous structure could be observed, due to the small vibration bands of CO₂ molecules [18]. At 1000 °C, less-porous structure was noticed [19], and no formation of CaO at temperature more than 1000 °C [20].

Pliya and Cree [15] used eggshell powder (ESP) in cement mortar, and the compressive and flexural strengths were significantly lower than control mortar. This is because the ESP did not provide any reactivity and only acting as inert filler material [15,21]. Balamurugan and Santhosh [17] used 1% of ESP calcined at 550 °C (eggshell ash) as cement replacement, and found that the compressive strength was slightly increased by approximately 14%. The previous researchers revealed that the eggshell ash (ESA) could act as accelerator in cement concrete [17, 22]. Further study focus on the combine use of ESA and rice husk ash (RHA) as cement replacement and a reduction of both compressive and flexural strengths were observed at different ages up to 28 days [23]. Similar finding was also reported by Beck et al. [24]. In chemical composition of cement, it was found the tricalcium silicate, dicalcium silicate, tetracalcium aluminoferrite, and tricalcium aluminate are the main compounds. In the eggshell ash, the dominating compound was the CaCO₃ and during the calcination, the CaCO₃ decomposed to CaO and gas of CO₂. When CaO reacts with H₂O that penetrates the concrete it forms a solution of Ca(OH)₂. It's well known the initial and final setting time of cement significantly influenced by selective hydration of the cement compounds. The cement hydration process at the early age was dominated by the tricalcium silicate and dicalcium silicate [17,22]. Since the main chemical composition of eggshell is CaO, it was strongly believed that the high calcium oxide amount accelerated the initial and final setting time of cement. However, the mechanisms of the reactions leading to the accelerating effect of eggshell content on the hydration of cement and the role CaO plays in inducing rapid hydration in cement. The high level of CaO in cement matrix provides additional dense gels such as calcium silicate hydrate, and calcium hydroxide for the rapid consumption of tricalcium silicate in the cement which resulted in the acceleration of hydration of the cement [15]. Hence the intimal and final setting time of the cement was trend to decrease with inclusion extra calcium oxide. Palm oil fuel ash (POFA) is one of the reactive pozzolanic materials that has potentiality to be used in cement concrete. However, the POFA concrete had long maturity strength development as compared to the normal concrete, therefore the accelerator could help in this case to accelerate or improve the early age of concrete strength.

Due to lack of knowledge especially about the potential use of ESP as accelerator in concrete, this paper aims to study and understand the performance of ground POFA (GPOFA) combined with 'high-energised' bio-lime derived from eggshell as accelerator in cement concrete. Transformation phase of ESP from CaCO₃ to CaO is investigated in order to identify which phase attributes to accelerator behaviour and provide reactivity to the cementitious materials. Three categories of ESPs namely, uncarbonised ESP (UC-ESP), carbonised ESP (C-ESP) and decarbonised ESP (DC-ESP) were prepared and studied using particle size analyser (PSA), scanning electron microscope (SEM/EDX), x-ray fluorescence (XRF) and loss of ignition (LOI), x-ray diffraction (XRD) and

fourier transform infrared (FTIR) spectroscopy. The reactivity of the ESPs was also examined using electrical conductivity. Finally, the feasibility of using ESPs as green accelerator in GPOFA concrete on the fresh properties, hydration and mechanical strength was demonstrated.

2. Experimental program

2.1. Raw materials

2.1.1. Ordinary portland cement

Ordinary CEM I Portland cement (OPC) was used as main hydraulic binder. The particle size distribution and chemical composition of OPC are shown in Fig. 1 and Table 1.

2.1.2. Palm oil fuel ash (POFA)

Palm oil fuel ash (POFA) is a local agriculture waste obtained from the southern part of Peninsular Malaysia. In this study, the POFA was first oven-dried at 100 °C for 24 h prior grinding and the particle size are tabulated in Fig. 1. Based on the total content of SiO₂, Fe₂O₃ and Al₂O₃, the ground POFA (GPOFA) can be regarded as Class C pozzolan [25–27]. The chemical composition of GPOFA is presented in Table 1. It was observed that OPC and GPOFA possessed major components differently, in which OPC contained 60% of calcium oxide (CaO) while GPOFA yields 53.30% of silicon dioxide (SiO₂). The presence of higher silica content in POFA has proven the pozzolanic properties of this material in comparison to the lower percentage of silica in OPC. It was a beneficial effect to have high silica content for the enhancement of pozzolanic reaction due to the formation of C-S-H gels which further strengthened the concrete. There are also other compounds such as magnesium oxide, potassium oxide, ferric oxide, aluminium oxide, phosphorus pentoxide and sulfur trioxide. These elements were amounting 10% for OPC and 16% for POFA, respectively. The carbon content present in the fuel ash or any other ashes varies and dependent on the combustion process. The loss on ignition (LOI) for GPOFA was slightly higher than OPC, which was about 12%. It was in accordance with the maximum value range stipulated in ATM C618 for both class C and class F pozzolans.

2.1.3. Eggshell

Chicken eggshell waste used in this study was sourced from local industry located at southern part of Peninsular Malaysia. The collected eggshell waste was washed with clean water followed by an oven drying process at 100 °C for 24 h. Then, the eggshell waste was ground to obtain particles with size less than 45 µm. The original ESP was put through a modification process whereby the calcination process was continued before grinding using the Shimpo ball mill machine. For the C-ESP and DC-ESP production, the calcination process was continued before grinding using Shimpo ball mill machine. Firstly, 200 g of ESP was weighed in each crucible before the calcination in the furnace. For C-ESP, it was calcined (heated) at 750 °C for 1 h while the DC-ESP was calcined at 1000 °C for 1 h. After the C-ESP and DC-ESP were calcined in the furnace, these ESP were then stored in the desiccator with silica gel. Next, the C-ESP and DC-ESP were grinded using Shimpo ball mill machine, whereby 500 g of ESPs was weighed in each drum and the duration was 3 h. In this phase, C-ESP and DC-ESP with fineness of 45 µm were obtained. All these C-ESP and DC-ESP were kept in a desiccator with silica gel to ensure good condition after calcination or grinding processes. The colour of the produced eggshell powder, i.e. UC-ESP, C-ESP and DC-ESP are illustrated.

It can be seen from Fig. 2 that the calcination process changed the original ESP from milky (white-light yellowish) colour to light grey after exposure to 750 °C for 1 h associated to the carbon realise (by 55 wt%). At 1000 °C, the colour became a clear white or colourless crystal after decarbonation process. To evaluate the thermal treatment effect on chemical and mineral properties of prepared eggshell, X-ray Fluorescence (XRF), X Ray diffraction (XRD) and Fourier Transform Infrared Spectroscopy (FTIR) tests are contacted.

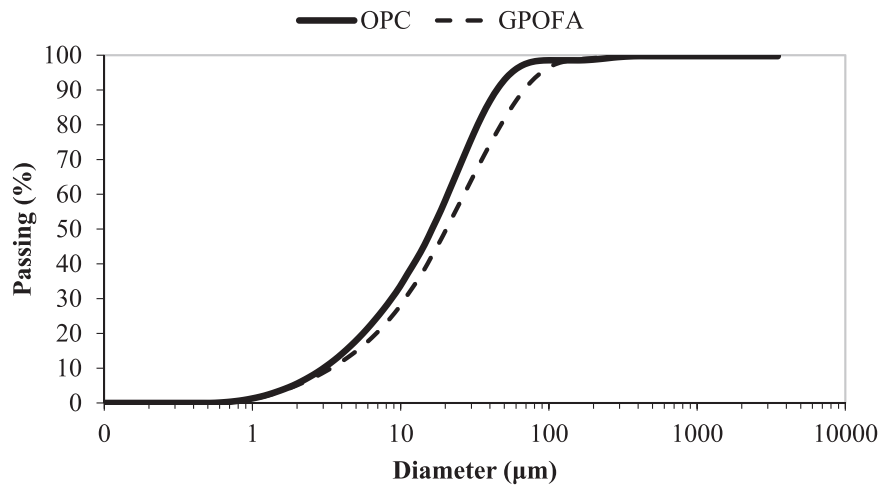


Fig. 1. Particle size distribution of ground palm oil fuel ash.

Table 1
Chemical composition of OPC and GPOFA.

Chemical oxide	OPC	GPOFA
Silica oxide, SiO ₂	14.60	53.30
Magnesium oxide, MgO	0.62	4.10
Calcium oxide, CaO	60.00	9.20
Pottasium oxide, K ₂ O	0.84	6.10
Ferric oxide, Fe ₂ O ₃	2.20	1.90
Aluminium oxide, Al ₂ O ₃	3.34	1.90
Sulfur trioxide, SO ₃	2.63	-
Phosphorus pentoxide, P ₂ O ₅	-	2.40
Summation of SiO ₂ , Fe ₂ O ₃ , Al ₂ O ₃	20.14	57.10

2.1.4. Aggregates

Natural river sand and gravel were used as fine and coarse aggregates in the preparation of concrete specimens. The size of fine and coarse aggregates having particle size of less than 5 mm (fineness modulus of 2.4) and 10 mm was used, respectively.

2.2. Physical and chemical tests for ESP

It is important to identify the physical and chemical changes of ESP before and after exposure to different calcination temperatures. The particle size distribution of ESP dispersed in liquid was analysed using the laser diffraction technique. The microstructure morphology and elemental were observed by scanning electron microscope (SEM/EDX) under a magnification of 5000 × . The chemical oxides of three categories of ESPs was examined using x-ray fluorescence (XRF). The loss on ignition (LOI) was conducted to measure the unburnt carbon content and organic matter of ESP samples up to temperature of 750 °C.

Mineralogical of ESP samples were analysed using X-ray diffraction (XRD) with current and voltage intensity of 40 kV and 18 mA. The XRD data were collected in the angular range of 10 ≤ 2θ ≤ 100° with scanning speed of 2 °/min. Fourier transform infrared (FTIR) spectroscopy was also employed to understand the functional groups of ESP samples. The test was conducted using a spectrum wavelength in the range of 400–4000 cm⁻¹ at a resolution of 4 cm⁻¹ and accumulations of 10 scans.

2.3. Reactivity of raw materials by electrical conductivity

To understand the reactivity of ESP samples, a rapid evaluation technique was conducted by measuring the electrical conductivity of binder materials suspended in Ca(OH)₂ solution [28,29]. The test was initiated with the preparation of Ca(OH)₂ solution in a beaker; 200 mg of analytical-grade Ca(OH)₂ diluted with 250 ml distilled water at controlled temperature of 40 °C. The raw material was weighed about 5 g and added into lime water system in the same beaker after reached a constant conductivity reading. The material together with lime water system was immediately stirred by using magnetic stirrer until complete designed duration of 250 min. To get the readings, two types of probes were insert into the mixed solution; digital of electrical conductivity and pH meter.

2.4. Concrete specimens and test methods

Tables 2–4 summarize the sixteen mix proportions of concrete containing GPOFA and ESPs with 0%, 5%, 10%, 15%, and 20% by weight of cement replacement. To achieve compressive strength of 30 MPa at 28 days, 455 kg/m³ OPC was used; and the fine and coarse aggregates were fixed at 905 kg/m³ and 740 kg/m³, respectively. For all the mixtures,

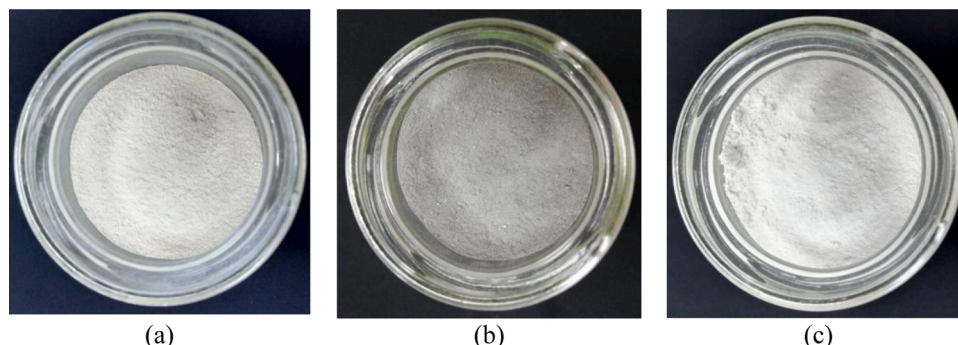


Fig. 2. Physical Features (a) UC-ESP (b) C-ESP (c) DC-ESP.

Table 2

Notation and replacement percentage of GPOFA with UC- ESP.

Concrete Type	Mix Design		Notation
	GPOFA (%)	ESP (%)	
Normal Concrete	-	-	NC
GPOFA with UC-ESP	20	0	G20UC0
GPOFA with UC-ESP	15	5	G15UC5
GPOFA with UC-ESP	10	10	G10UC10
GPOFA with UC-ESP	5	15	G5UC15
GPOFA with UC-ESP	0	20	G0UC20

Table 3

Notation and replacement percentage of GPOFA with C- ESP.

Concrete Type	Mix Design		Notation
	GPOFA (%)	ESP (%)	
Normal Concrete	-	-	NC
GPOFA with C-ESP	20	0	G20C0
GPOFA with C-ESP	15	5	G15C5
GPOFA with C-ESP	10	10	G10C10
GPOFA with C-ESP	5	15	G5C15
GPOFA with C-ESP	0	20	G0C20

Table 4

Notation and replacement percentage of GPOFA with DC-ESP.

Concrete Type	Mix Design		Notation
	GPOFA (%)	ESP (%)	
Normal Concrete	-	-	NC
GPOFA with DC-ESP	20	0	G20DC0
GPOFA with DC-ESP	15	5	G15DC5
GPOFA with DC-ESP	10	10	G10DC10
GPOFA with DC-ESP	5	15	G5DC15
GPOFA with DC-ESP	0	20	G0DC20

the water to cement ratio was kept at 0.55 with no superplasticizer. The fresh concretes were poured and cured in moulds for 1 day before subjected to further water curing. After 7 days of water curing, the specimens were taken out and left in the lab temperature (24 ± 3 °C) until the testing. All samples were strictly prepared according to BS EN 12390–2: 2000 [30].

In the fresh state, workability of GPOFA concrete mixtures containing different content of ESPs were employed using a conventional slump cone method. To understand the performance of ESP as green accelerator in GPOFA concrete, a modified hydration test similar to that of previous works [31,32] was conducted (see Fig. 3). Type-K thermocouple was embedded into fresh concrete samples placed in a plywood box shielded with polystyrene as thermal insulation. The thermocouples were connected to a data logger and the exothermal temperature due to cement hydration was recorded every 10 mins for 30 h.

In the hardened state, compressive strength of 100 mm cube

concrete samples was determined after 1, 3, 7, 28, 56 and 90 days of curing ages. An universal compression testing machine with a load capacity of 200 kN set at loading rate of 6 kN/s was used. Three samples for each mix design was tested and average results were reported.

The morphology of raw materials in powder form, the sample of NC and optimum GPOFA with ESPs sample pastes at ages of 3 and 56 days were investigated by using Scanning Electron Microscopy (SEM). First, (a) the powder form was sowed onto the double cellophane which was attached to the small coin. Then, (b) all the specimens were coated using the gold sputter coater machine before the morphological testing. All specimens were placed inside the drift detector that offers superior speed and energy resolution. The SEM device Brand Hitachi Model S-3400 N was used. Finally, (d) the significant morphology image was captured with sufficient magnifications.

The strength activity index (SAI) for optimum mix proportion of GPOFA with ESPs was checked for its pozzolanic properties, as prescribed by 'Standard Test Methods for Sampling and Testing Fly Ash or Natural Pozzolans for Use in Portland-Cement Concrete. The SAI could be calculated using Eq. 1. The specimens at different ages were tested and the average value was calculated and considered for future analysis.

$$\text{Strength Activity Index (SAI)} = \frac{A}{B} \times 100 \quad (1)$$

Where,

A is an average compressive strength of optimum mix proportion specimen (MPa).

B is an average compressive strength of control specimen (MPa).

3. Results and discussion

3.1. Calcination of ESPs

3.1.1. Particle size distribution

Fig. 4 shows the particle size distribution of ESPs before and after calcination at 750 °C and 1000 °C. It was found that all the ESPs showed well graded particle size ranged from 0.2 to 100 µm. Approximately 80% of ESPs had passed through the sieve size of 45 µm which is close to cement grain size [27]. In comparison, DC-ESP calcined at 1000 °C showed finest in particle size when comparing with UC-ESP and C-ESP. According to Jazie et al. [19], the particle size decreased with an increase of calcination temperature up to 1000 °C due to severe reduction of unit cell after a complete decarbonation [33,34].

3.1.2. Scanning electron microscope (SEM/EDX)

Fig. 5 shows the SEM images of ESPs before and after calcination at different temperatures. Prior to thermal treatment, the UC-ESP particles were present in irregular shape (see Fig. 5a). After being subjected to 750 °C for 1 h, the physical morphology of the ESP interconnected to each other and filled up some of the original pores (see Fig. 5b). This reflects that part of the carbon content has been removed from the ESP particles. When the calcination temperature increases up to 1000 °C, all the carbon content was expected to remove completely and the physical



Fig. 3. Hydration test (a) thermocouple inserted in fresh concrete (b) test setup.

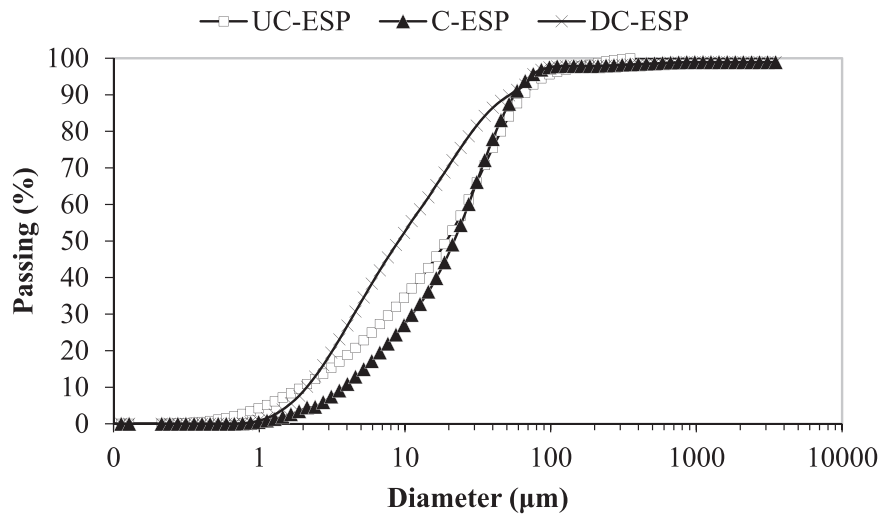


Fig. 4. Particle size distribution of eggshell powder (ESP) before and after calcination.

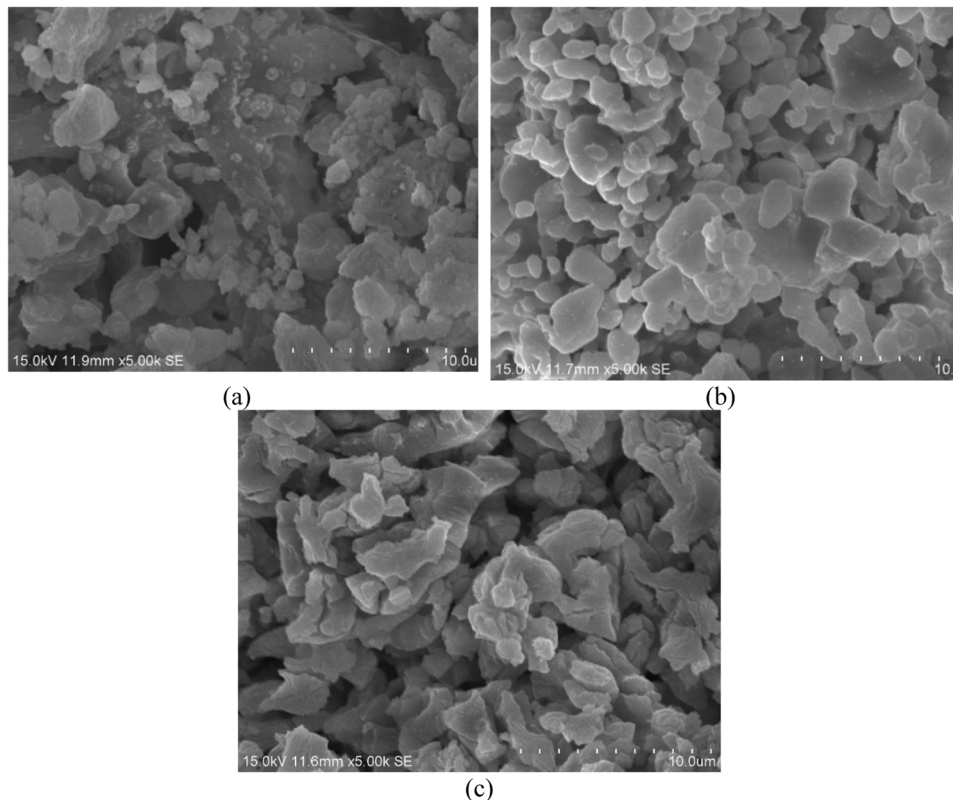


Fig. 5. Morphology images (a) UC-ESP (b) C-ESP (c) DC-ESP.

structure became a ‘sharp-skeleton’ shape (see Fig. 5c). The presence of carbon content was also revealed in LOI results shown in Table 6. Additionally, the evidence of crystalline shape of DC-ESP relatively to the particle size as presented in Fig. 4; crystalline size of DC-ESP leads to have smallest size as compared to particle size of UC-ESP and C-ESP.

3.1.3. X-ray fluorescence (XRF) and loss on ignition (LOI)

The chemical compositions of ESPs obtained from XRF test and LOI content are summarized in Table 5. The calcium content of ESP was obviously increased when the ESP exposed to higher calcination temperature. Both UC-ESP and C-ESP had approximately 70% of calcium content, while 98% of calcium content was recorded for DC-ESP. This is

Table 5
Chemical composition and LOI at different categories of ESPs.

Chemical composition (%)	UC-ESP	C-ESP	DC-ESP
Silica oxide, SiO ₂	0.04	< 0.01	0.01
Magnesium oxide, MgO	0.36	0.36	0.07
Calcium oxide, CaO	68.54	70.03	98.20
Pottasium oxide, K ₂ O	0.06	0.06	< 0.10
Ferric oxide, Fe ₂ O ₃	0.12	0.11	0.30
Aluminium oxide, Al ₂ O ₃	< 0.01	0.04	< 0.10
Phosphorus pentoxide, P ₂ O ₅	-	-	-
Sulfur trioxide, SO ₃	0.68	0.29	0.01
Loss on ignition, LOI	-	47.40	3.00

because some impurities had been totally removed at 1000 °C calcination temperature. For instance, the impurities of magnesium oxide and sulphur trioxide were significantly reduced in the case of DC-ESP. In the LOI results, it was also demonstrating that the C-ESP had the highest LOI content (47%) due to the higher organic matter and carbon content. These findings also agreed with the fact that both UC-ESP and C-ESP relative to CaCO₃, while, DC-ESP relative to CaO. The enhancement on CaO content and reduction on LOI level of DC-ESP powder significantly increased the reactivity of ESP and reaction process during the modified cement hydration.

3.1.4. X-ray diffraction (XRD)

According to the XRD results shown in Fig. 6, either with and without calcination all the ESP samples demonstrating strong crystalline structures. Almost similar peaks were clearly identical in UC-ESP and C-ESP samples, approximately 70% were CaCO₃ aligned at 30°, 37°, 40°, 44°, 47°, 49° 2-Theta scale. However, the C-ESP showed higher intensity peak at 30° 2-Theta scale, indicating C-ESP is being to form intermediate phase from CaCO₃ to CaO. In contrast with UC-ESP and C-ESP, the main 8 peaks identified at 33°, 38°, 54°, 64°, 67°, 80°, 89°, 92° 2-Theta scale for DC-ESP sample were corresponding to CaO (98%). This confirm that at 1000 °C, the CaCO₃ has been fully transformed into CaO. Other study [20] reported that increasing the temperature more than 1000 °C showed no increment in CaO content. The changing of chemical phases was attributed as an evidence that reflect to the DC-ESP have become porous, fragile and crystal-white colour.

3.1.5. Fourier transform infrared (FTIR) spectroscopy

The FTIR patterns of ESPs are shown in Fig. 7. Three characteristic peaks occurred at 1422, 875, and 712 cm⁻¹ indicating the occurrence of calcite (CaCO₃) in UC-ESP. A very intense absorption bands at 875 and 712 cm⁻¹ are attributed to, CO₃ bending out-of-plane deformation (ν_2), and OCO bending in-plane deformation (ν_4) mode vibrations while peak at 1422 cm⁻¹ was observed for asymmetric C-O stretching (ν_3). The absorption bands around 3200–3600 cm⁻¹ is due to the stretching vibration of water molecules [35]. Similar pattern on the IR absorption bands was observed upon calcination temperature at 750 °C. However, the C-ESP showed a relative lower intensity peak as compared to

UC-ESP. Similar reduction trend also indicated in the XRD finding, which is believed the C-ESP is being to form intermediate phase from CaCO₃ to CaO.

Upon decarboxylation at 1000 °C, ESP starts to lose carbonate and the relative intensities of CO₃²⁻ FTIR bands clearly decrease. The absorption bands of CO₃²⁻ molecules shift to higher energies ($\nu_3 = 1450 \text{ cm}^{-1}$, $\nu_2 = 1076 \text{ cm}^{-1}$, $\nu_4 = 874 \text{ cm}^{-1}$) indicates the transformation of CaCO₃ to CaO. This has been ascribed to the decrease of the reduced mass of the functional group connected to the CO₃²⁻ ions [12]. On the other hand, the absorption band of water molecules decreases with increasing temperature. The existence of peak at 3632 cm⁻¹ corresponds to the OH stretching mode during adsorption of water by CaO indicates a low concentration of Ca(OH)₂ in the sample [36]. The absence of a sharp absorption frequency from 700 to 900 cm⁻¹ indicates that the calcite (CaCO₃) as the basic components of the eggshell are no longer present as it already converted to CaO. This was also proved by the existence of absorption characteristic for metal oxide, CaO at 546 cm⁻¹ [37]. The vibration modes and absorption bands at different categories of ESPs were summarized in Table 6.

3.2. Reactivity behaviour of ESPs

Fig. 8 shows the conductivity-time behaviour of cement, GPOFA and ESPs, and a higher the conductivity indicates a lower reactivity in lime water system. As it can be seen, similar plateau conductivity behaviour was observed for all the tested materials. However, the DC-ESP showed the highest reactivity followed by cement, C-ESP, UC-ESP and GPOFA. The superior reactivity owned by DC-ESP can be explained by the dissolution of CaO to form Ca(OH)₂. Since the lime water system is existing in Ca(OH)₂ solution, it become binary-reactivity of DC-ESP in lime water system. In contrast, GPOFA, UC-ESP and C-ESP seem to have very low reactivity in lime water system due to the present of inert and stable CaCO₃.

The absolute loss in conductivity-time behaviour of these materials are present in Fig. 9. The degree of cementitious and pozzolanic reactivity can be explained at this stage. In this case, certain materials had gradually increased the loss in conductivity when the time was increased and certain materials seem had plateau behaviour of loss in

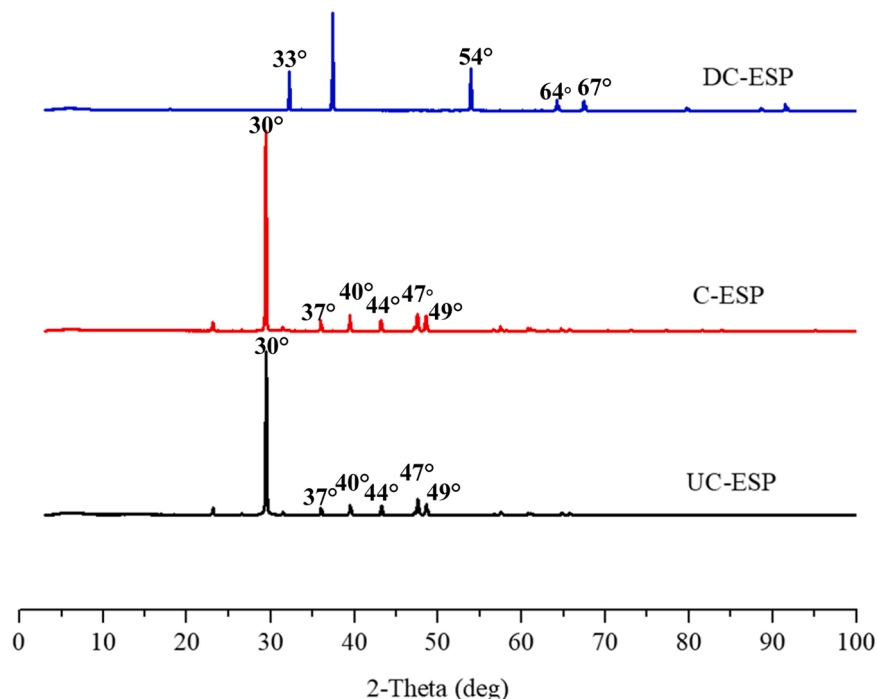


Fig. 6. XRD analysis for UC-ESP, C-ESP and DC-ESP.

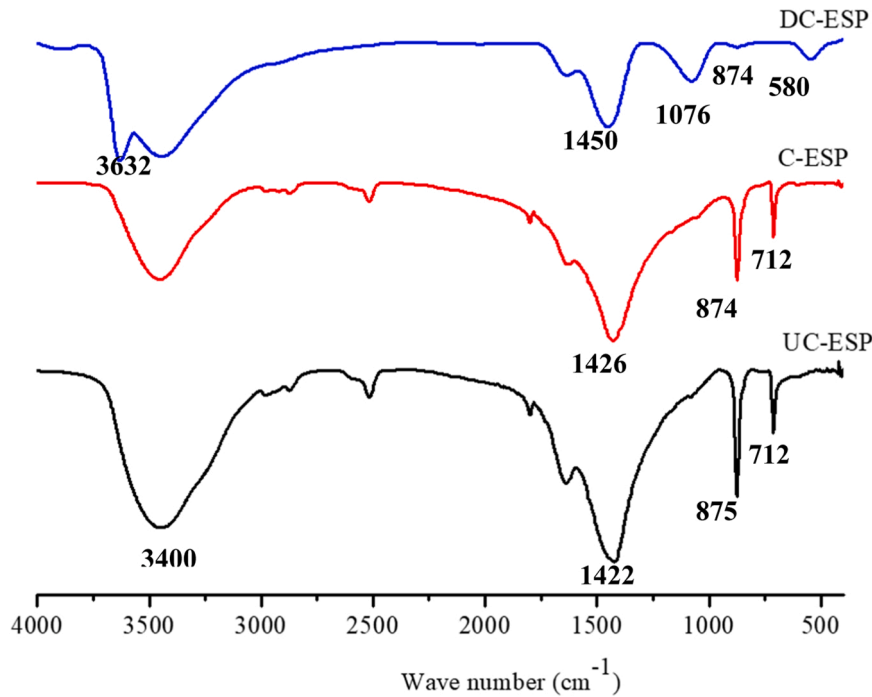


Fig. 7. FTIR analysis for UC-ESP, C-ESP and DC-ESP.

Table 6
Vibration modes and absorption bands at different categories of ESPs.

This work		Ref [38]	This work	Ref [18]	Assignment
UC-ESP $\bar{\nu}$ (cm ⁻¹)	C-ESP $\bar{\nu}$ (cm ⁻¹)	$\bar{\nu}$ (cm ⁻¹)	DC-ESP $\bar{\nu}$ (cm ⁻¹)	$\bar{\nu}$ (cm ⁻¹)	
712	712	712	874	820	ν_4 -Symmetric CO ₃ deformation
875	874	876	1076	1040	ν_2 -Asymmetric CO ₃ deformation <i>In-plane bending</i>
1422	1426	1435	1450	1470	ν_3 -Asymmetric CO ₃ stretching <i>Out-of-plane bending</i>

conductivity. However, the higher absolute loss in conductivity gives insight that the higher cementitious or pozzolanic reactivity in lime water system. As known, when the cement reacts with water, it produced C-S-H gel and Ca(OH)₂, that is the reason explaining cement

reactivity is superior (approximately 45% loss in conductivity) as compared to others especially in lime water system. In this case, the cement reactivity occurred as fast as at 20 mins from overall conductivity time frame. As for the GPOFA, it seems to have pozzolanic reactivity (about 19% loss in conductivity), and the finer the POFA the better is the pozzolanic reactivity [32]. While, by comparing loss in conductivity among ESPs, the DC-ESP had performed high reactivity (about 7% of loss in conductivity) as compared to the UC-ESP and C-ESP. As explained, the presence of CaO derived DC-ESP in water provide the formation of Ca(OH)₂; offer binary-reactivity of CaO especially in lime water system. In addition, overall materials had performed in pH alkali condition which it performed more than pH of 7 as shown in Fig. 10. This finding further ensured that the combination between GPOFA and DC-ESP is possible in order to provide SiO₂-CaO reactivity as green accelerator especially in cement concrete.

3.3. ESP in GPOFA concrete

3.3.1. Workability

The workability of GPOFA concrete containing different percentage

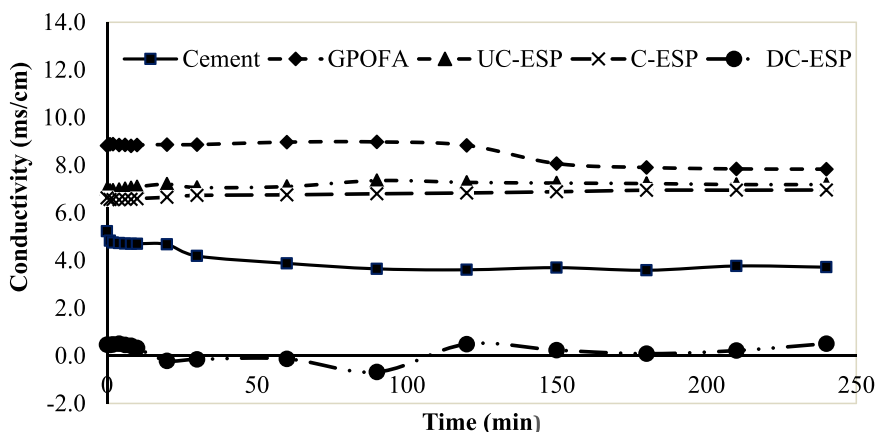


Fig. 8. Conductivity-time behaviour of cement, GPOFA, ESPs in lime water system.

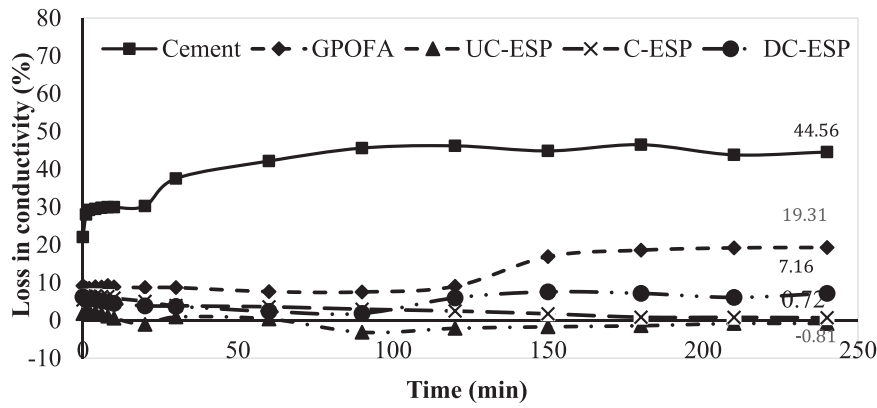


Fig. 9. Loss in conductivity-time behaviour of cement, GPOFA, ESPs in lime water system.

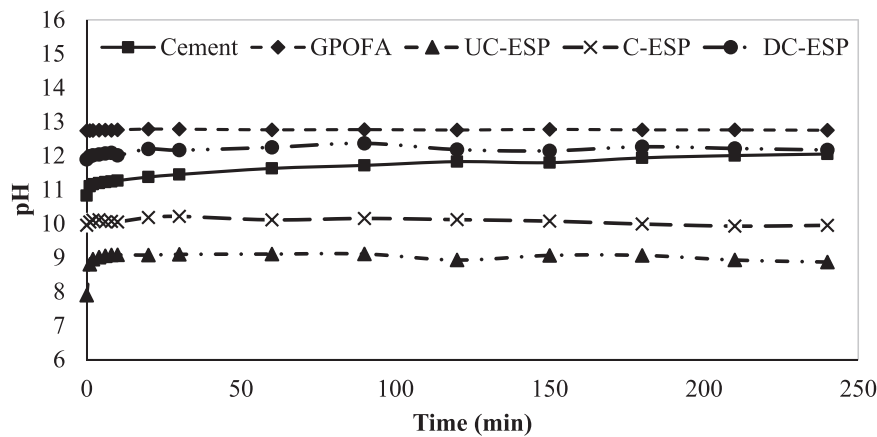


Fig. 10. pH behaviour of cement, GPOFA, ESPs in lime water system.

and categories of ESPs is presented in Fig. 11. Regardless of replacement content, the GPOFA concrete containing ESPs showed lower workability as compared to NC. Among them, GPOFA concrete with DC-ESP had lowest workability due to its very fine particles (see Fig. 4) and larger specific surface area [32]. However, the overall workability of concrete was acceptable within the designed target slump of 60–180 mm (marked with dotted line as reference line) for most construction applications.

3.3.2. Hydration behaviour

Fig. 12 shows the hydration behaviour of normal concrete (NC) compared with concrete containing solely percentage of GPOFA (G20), ESPs (UC20, C20 and DC20) and selected mix concrete up to 30 h. The rise of hydration temperature depicts to the initial cement reactivity and it was obvious that high hydration temperature occurred for concrete containing solely DC-ESP (approximately reached 47 °C) as compared to other type of concretes (reached in between 33 and 37 °C). The rapid

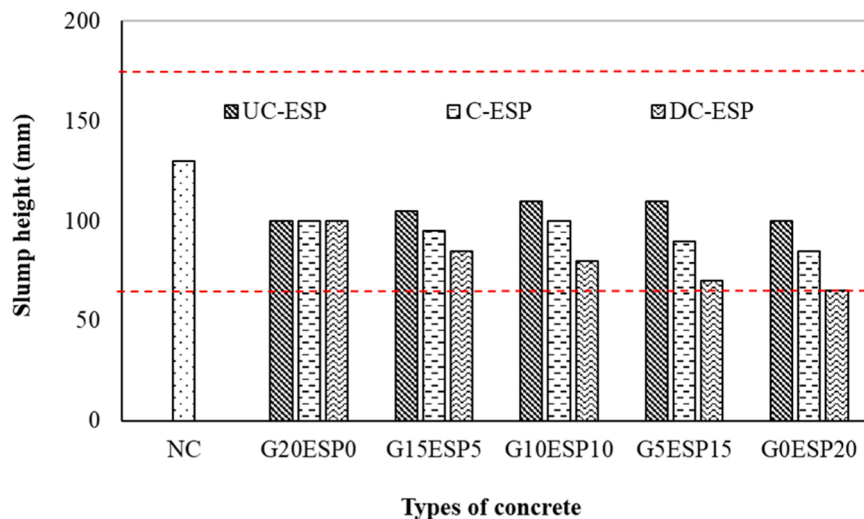


Fig. 11. Workability of GPOFA concrete containing different categories of ESPs.

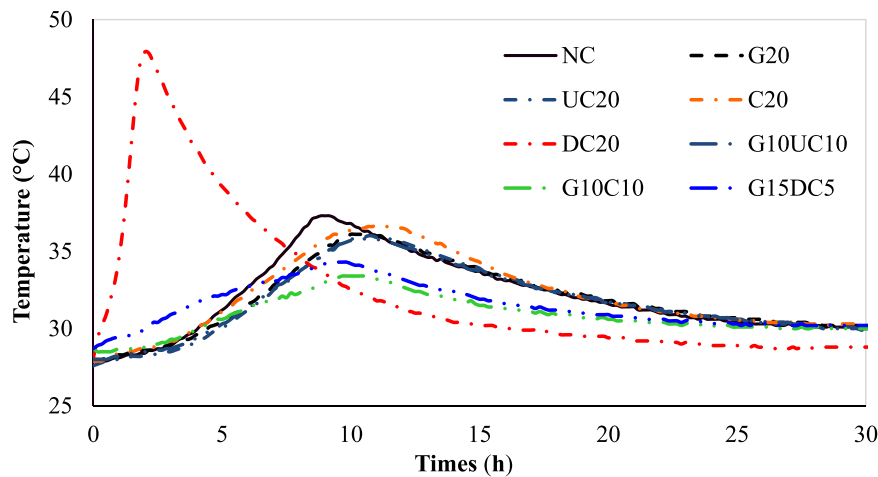


Fig. 12. The hydration behaviour of GPOFA concrete containing different categories of ESPs.

hydration of concrete containing solely DC-ESP results in flash setting. The flash setting normally reflect to the quick condition that cause to the unworkable concrete. Too high of hydration temperature with flash setting phenomenon could cause to the expansion to concrete and leads to occurrence of unseen concrete’s hair cracks. The GPOFA concrete containing 5% of DC-ESP (G15DC5) had lower hydration temperature, and slightly comparable to the G10C10 as compared to the NC. However, G15DC5 concrete gradually served inductive hydration temperature initiated at 29 °C to 32 °C within 5 h; obviously provide accelerator reactivity to the concrete. In this case, the rapid hydration and inductive hydration happened due to the formation of Ca(OH)₂ derived from CaO (DC-ESP).

3.3.3. Compressive strength

Compressive strength of GPOFA concrete containing different percentage of ESPs at different curing age is shown in Figs. 13, 14 and 15. At 1 day, the utilization of solely UC-ESP in concrete showed no contribution in early age strength development, but for the case of solely C-ESP and DC-ESP the strength was increased by about 20% and 30%, respectively. In other words, UC-ESP, C-ESP and DC-ESP showed low, medium and superior accelerator action in GPOFA concrete, respectively. The presence of CaCO₃ derived UC-ESP and C-ESP being as inert materials and the presence of CaO derived DC-ESP could react as a reactive material with the presence of pozzolan in the GPOFA concrete.

Regardless of curing age, for the case of concrete mixes containing UC-ESP and C-ESP the highest strength (optimum mix) was observed

when 10% of the respective ESP was incorporated with 10% GPOFA. However, for the case of DC-ESP, the utilization of 15% GPOFA and 5% of DC-ESP in concrete showed the highest strength at all curing ages. The combination materials of pozzolan (e.g. GPOFA) with ESPs were found to have a superior synergy-reactivity for both early and later age of concrete development. This is because when the SiO₂ react with CaO, it provides calcium silicate (Ca₂SiO₄) reactivity for strength enhancement [38,39]. In comparison, the GPOFA concrete containing C-ESP performed slightly better especially at the later age strength gain than other two ESPs, probably due to the presence of carbon in C-ESP as discussed early. The inclusion of G-POFA and DC-ESP significantly improved the failure mood of tested concrete specimens as shown in Fig. 16.

3.4. Scanning electron microscopy characteristics

The SEM and EDX analyses of the 5 types of paste specimens under 2 different curing ages, i.e. 3 days and 56 days of curing ages are shown in Figs. 17 to 26, respectively. Based on the observations, the SEM of normal paste (NP) and GPOFA paste mixtures have shown the formation of C-S-H gel. Invariably, the microstructure of the paste samples changed as the curing age progresses. It was apparent that NP mixture contains many crystalline structures, which interweaves together with C-S-H gel. Meanwhile, several voids are noticeable amongst these crystalline. Contrarily, the GPOFA paste mixture contains many gel components and contains lesser voids than normal paste mixture. As seen in Fig. 22 and Fig. 23, at the 56 days curing period, the C-S-H gel was more evenly

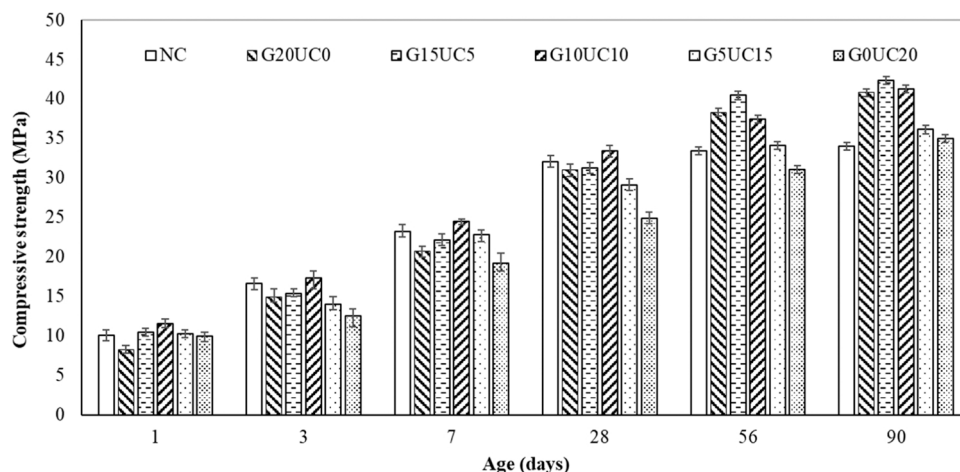


Fig. 13. Compressive strength of GPOFA concrete containing different percentage of UC-ESP at different curing age.

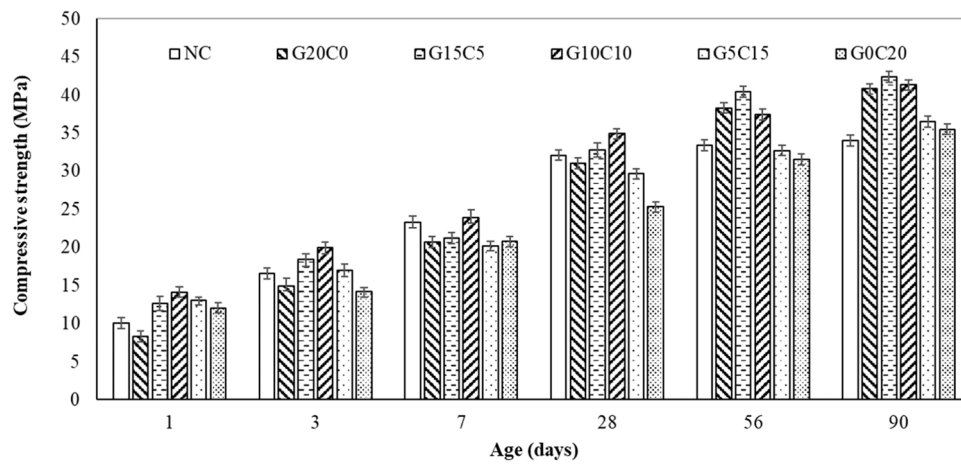


Fig. 14. Compressive strength of GPOFA concrete containing different percentage of C-ESP at different curing age.

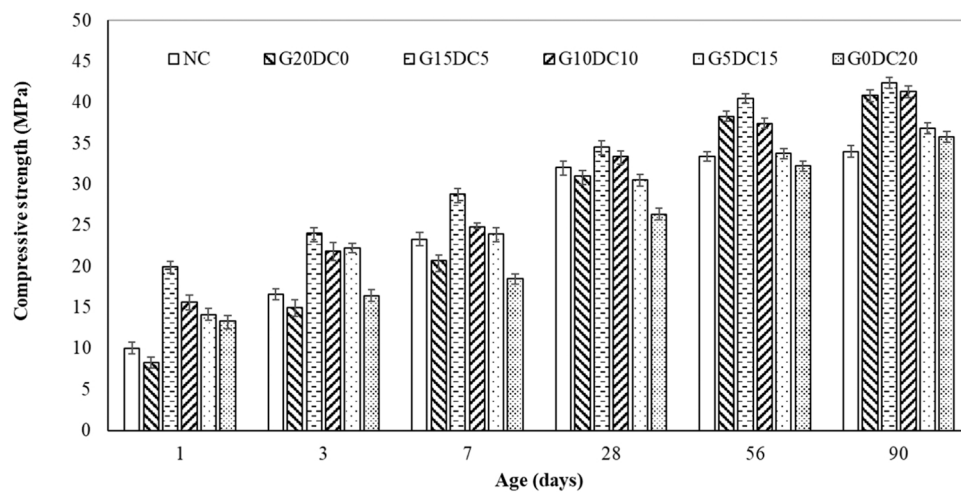


Fig. 15. Compressive strength of GPOFA concrete containing different percentage of DC-ESP at different curing age.

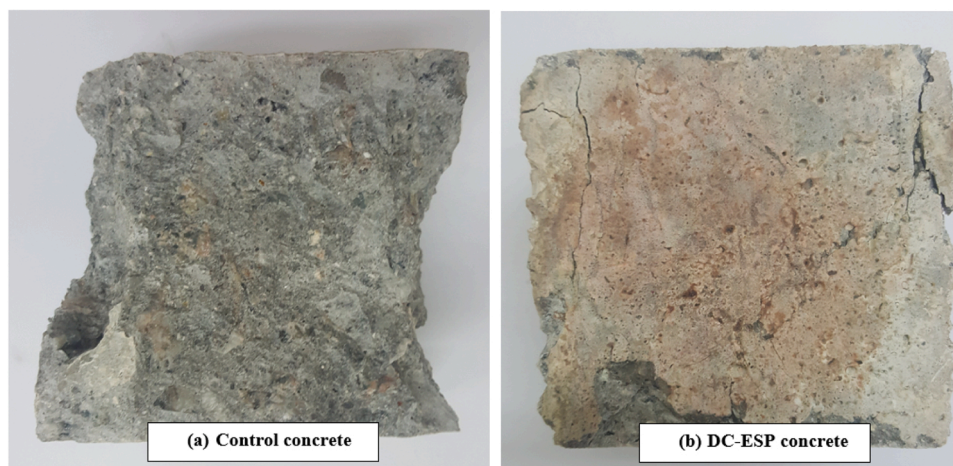


Fig. 16. Ultimate failure patterns of the tested cubes (a) control concrete (b) DC-ESP concrete.

spared in GPOFA paste over the NP. The finely spared of C-S-H gel and formation of extra C-S-H gel owed to the consumption of Portlandite by the pozzolanic action of GPOFA in the presence of moisture and resulted in better performance of the concrete mixtures in terms of strength and durability. This owed to the fact that POFA modified the concrete matrix

through the pozzolanic reaction and reduced the $Ca(OH)_2$ content. At curing period of 56 days, GPOFA concrete mixture has achieved higher compressive strength than that of NC content concrete mixtures as described in previous sections. Moreover, after a certain period of curing, the hydration products of the GPOFA are well developed and the

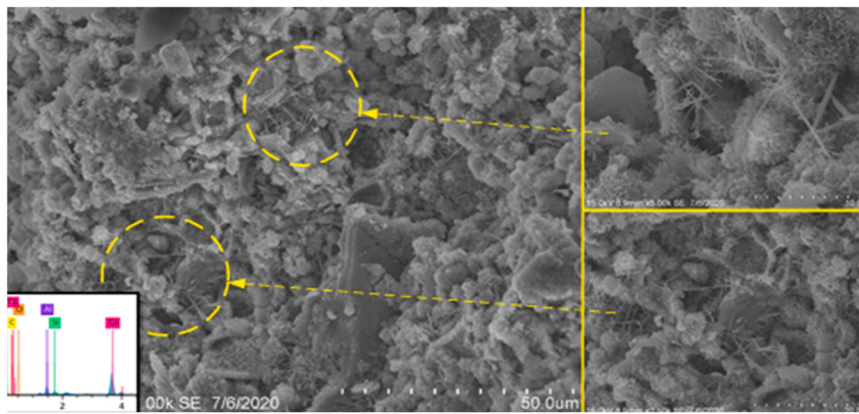


Fig. 17. SEM and EDX analysis for normal paste (NP) at curing age of 3 days.

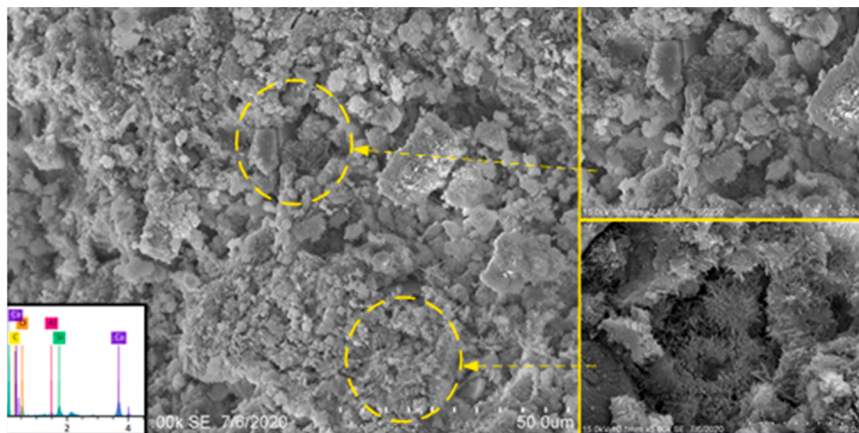


Fig. 18. SEM and EDX analysis for GPOFA paste at curing age of 3 days.

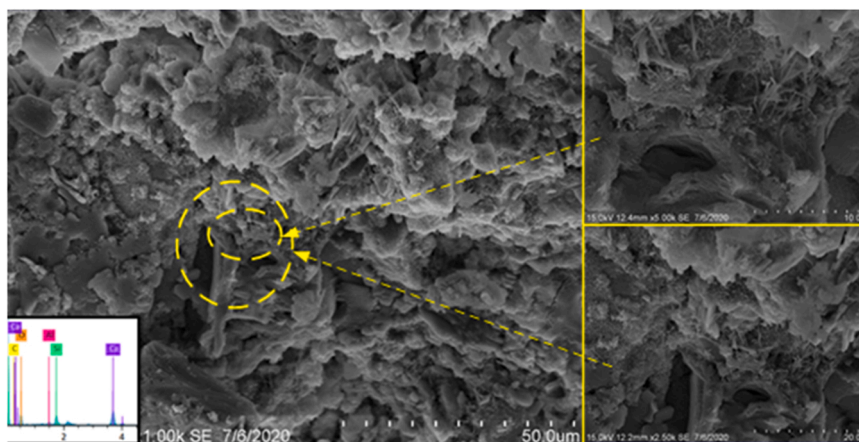


Fig. 19. SEM and EDX analysis for optimum GPOFA UC-ESP paste at curing age of 3 days.

structure of the GPOFA paste was shown to be comprised with GPOFA particle in the state of more advanced hydration. This has further proven that calcium hydroxide (CH) crystals have been consumed and transformed into C-S-H, which can be considered as the strength contributing phase.

Additionally, based on Figs. 19 to 21 and Figs. 24 to 26, it was shown that the optimum GPOFA UC-ESP paste had irregular and jagged morphology when there was no special heat treatment on the ESP. It was observed that the ESP has random size distribution with inconsistent

shapes of pores. When heat treatment was applied on the C-ESP, a more uniformly distributed open pores was demonstrated with some hollow pores between crystalline calcite to allow gaseous transfer within the ESP. This phenomenon was possibly due to the decomposition of organic matter when the temperature increased. As the temperature elevated to 1000 °C for DC-ESP, the morphology for optimum GPOFA DC-ESP paste was shown to have a uniform size and shape as well as smoother surface in comparison to other ESP. This was attributed to the complete transformation of CaCO_3 to CaO during this stage. The SEM images shown

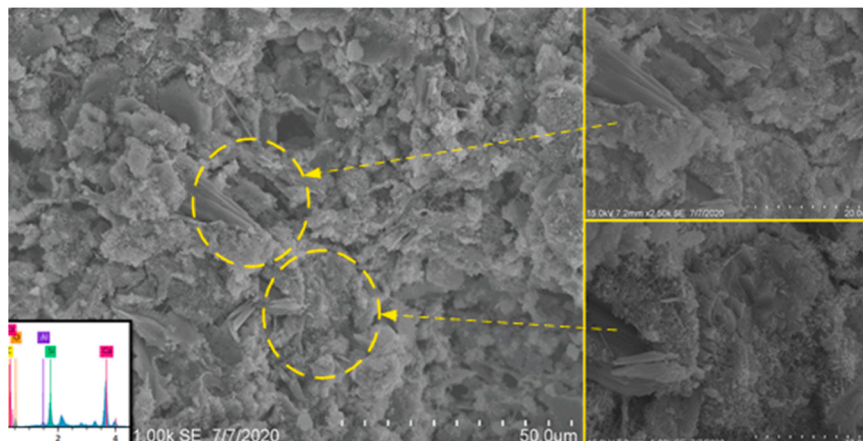


Fig. 20. SEM and EDX analysis for optimum GPOFA C-ESP paste at curing age of 3 days.

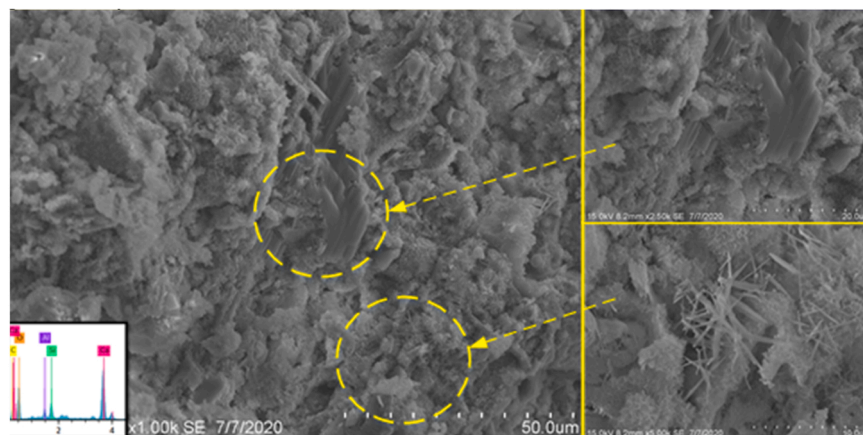


Fig. 21. SEM and EDX analysis for optimum GPOFA DC-ESP paste at curing age of 3 days.

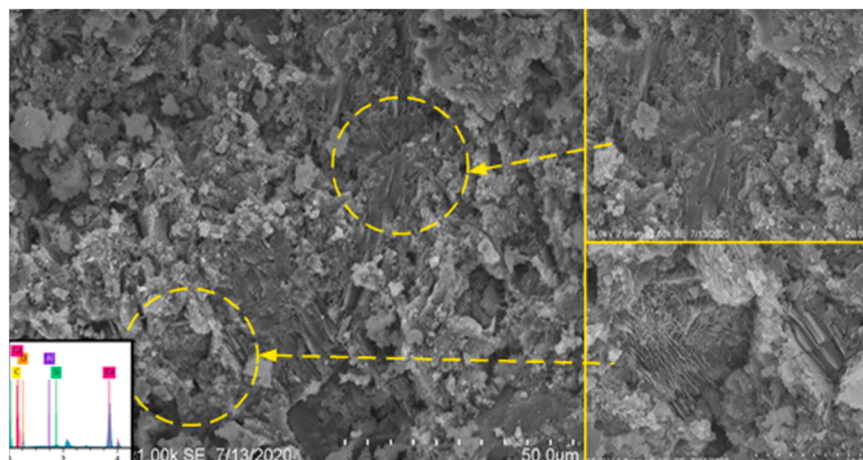


Fig. 22. SEM and EDX analysis for normal paste (NP) at curing age of 56 days.

after curing age of 56 days has demonstrated that the microstructures and cracks were reduced due to the increased strength and durability.

Apart from that, the EDX analysis also supported the findings of a high amount of SiO₂ and CaO element existing in GPOFA and ESP, respectively. The high silicon percentage detected in EDX was possibly due to the presence of silica as a main component in GPOFA. The EDX analysis also further confirmed the presence of high carbon percentage in the samples, which agreed with the typical charcoal particles

produced from the burning of cellulosic materials due to incomplete burning of carbon content originating from the cellulosic nature of GPOFA. Besides, it was exhibited that all three types of GPOFA-ESP paste specimen yield the highest content for CaO element, while optimum GPOFA DC-ESP paste presented with the highest percentage of CaO. This finding agreed with other analysis which presented the chemical composition in ESP. The EDX findings have proven the presence of the necessary pozzolans and accelerators materials in GPOFA-

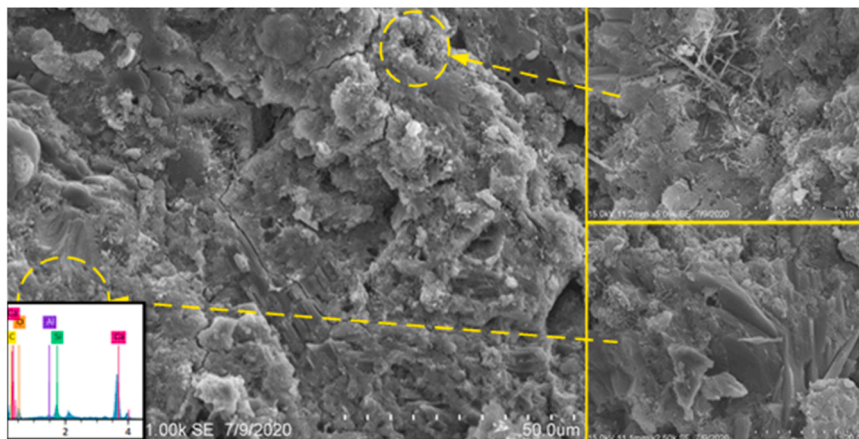


Fig. 23. SEM and EDX analysis for GPOFA paste at curing age of 56 days.

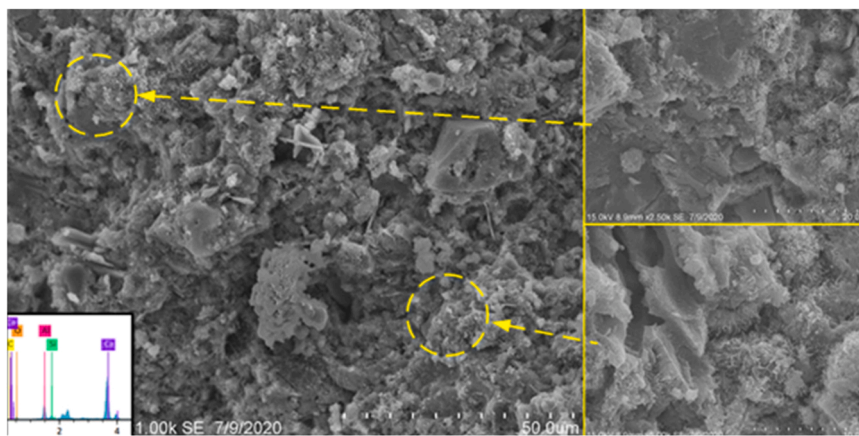


Fig. 24. SEM and EDX analysis for optimum GPOFA UC-ESP paste at curing age of 56 days.

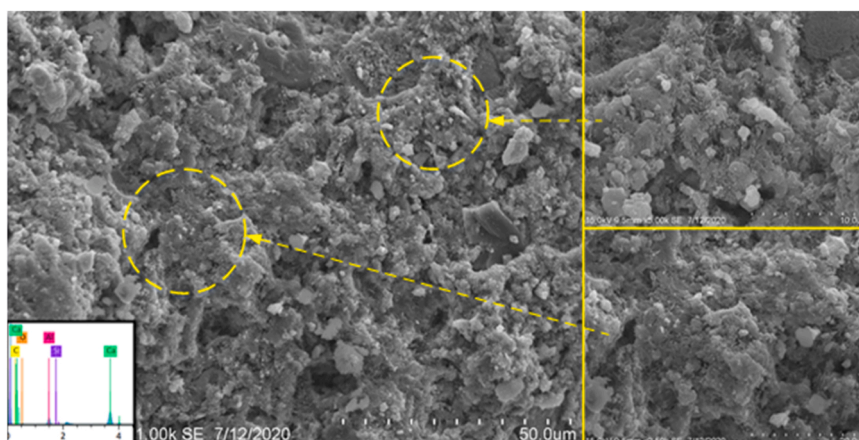


Fig. 25. SEM and EDX analysis for optimum GPOFA C-ESP paste at curing age of 56 days.

ESP pastes, which further validate and signify the importance and the versatility of these materials as the replacement of cementitious materials.

Therefore, it was deduced that the SEM image further revealed that the incorporation of GPOFA, alongside with the ESP, provided a homogeneous structure, which also led to the reduction in the size and number of the pores, while the EDX analysis has further proven the existence of relative content of carbonaceous materials, pozzolans, accelerators in the concrete mixtures. With that, it could be said that the

reduction in the cracks would result in improving the durability of concrete.

3.5. Strength activity index

The strength activity index (SAI) test is used to assess whether natural pozzolan results in an acceptable level of strength development when used with hydraulic cement in concrete. This test was adapted to determine the different strength values when the different percentage of

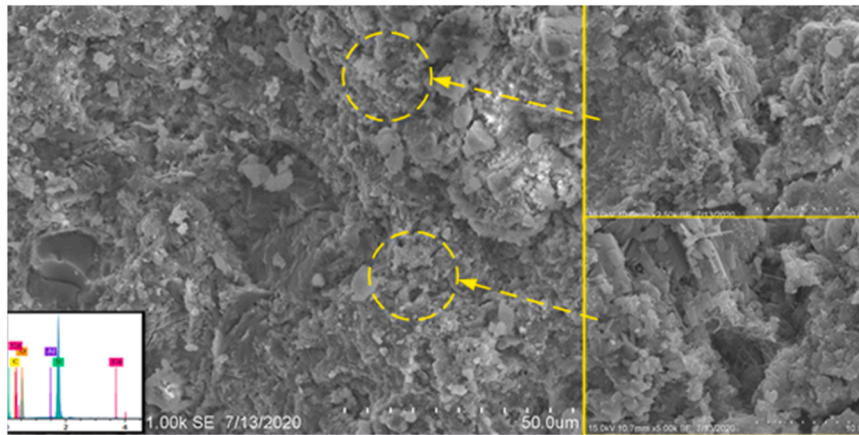


Fig. 26. SEM and EDX analysis for optimum GPOFA DC-ESP paste at curing age of 56 days.

replacement is used. As per stated in ASTM C311, the different percentage of replacement incorporated mortar is required to achieve 75% of SAI value to comply with the requirement for supplementary cementitious materials.

As shown in Figs. 27 and 28, the strength activity index for OPC (control sample), GPOFA and GPOFA-ESP mortar with various types of ESP was illustrated at a curing time of 7 days and 28 days. Based on the findings, it was observed that the strength activity indices at 7 and 28 days were exceeding the minimum permissible SAI of 75%. In comparison to the OPC as a reference, the optimum GPOFA-ESP mixtures, i.e. G10UC10, G10C10 and G5DC15 mortar exhibited a higher SAI percentage of 105, 103 and 123 for 7 days curing time while 104, 109 and 110 for 28 curing age, respectively. On the other hand, the replacement with solely GPOFA exhibited SAI percentage of 89 for 7 days while 97 for 28 curing age.

At the early age of 7 days, the SAI of G5DC15 mortar was seemed to be highest due to the acceleration effect of ESP as the early strength contributor while the decrement by GPOFA mortar was possibly attributed to the dilution effect which has delayed the pozzolanic reaction of GPOFA. At the later stage of the curing time of 28 days, the optimized GPOFA-ESP mixture sets have exhibited a higher SAI value due to the synergistic effect between ESP and GPOFA, which played their roles early strength and later strength developer to improve the concrete performance. The exact SAI value for all the optimized GPOFA-ESP concrete mixtures is shown in Table 7.

3.6. Stress-strain

The average stress-strain curve of NC, GPOFA and the optimum UC-

ESP, C-ESP and DC-ESP concrete at 28 days are presented in Fig. 29. The pattern of NC, GPOFA and concrete with different ESPs compressive strength were similar as discussed earlier (Section 3.3.3) where GPOFA-ESP concrete had superior compressive strength compared to NC and GPOFA concrete. the stress for each of the concrete sample was shown to be lowest for sample 2 (GPOFA concrete) at the curing age of 28 days in comparison to NC and the other 3 samples with ESPs. the concrete samples incorporated with the DC-ESP have exhibited higher stress compared to NC and GPOFA concrete. It was attributed to the advantages of DC-ESP which functions as accelerators. The gradual increment of optimum DC-ESP concrete was possibly due to the CaO purity of ESP. Strain at the failure of NC, GPOFA, optimum UC-ESP, C-ESP and DC-ESP concrete. All the five (5) concrete failed at the same local failure of about 2.2–2.3% of strain at 28 days of curing age. This situation gives insight that optimum DC-ESP concrete could sustain the applied load and prolong the deformation before it failed like NC. the GPOFA-UC-ESP concrete contains calcium carbonate (CaCO₃) which was regarded as an inert material or non-reactive calcium in the concrete. The calcination process would then convert CaCO₃ into CaO in C-ESP and thus increasing the amount of CaO as the accelerating materials in concrete, while the DC-ESP contains the highest amount of active CaO. Hence, the synergistic effect between GPOFA and the ESP with various CaO purity could provide dual functionality in the concrete strength enhancement, which resulted in the stress and strain trend as presented in Fig. 29. As it is known, when the cement reacts with water, it produces C-S-H gel and Ca(OH)₂. It means that calcium hydroxide occurred from this reaction when it was mixed together. In addition, the presence of CaCO₃ derived UC-ESP as inert materials and the presence of CaO derived C-ESP and DC-ESP could react as a reactive material with pozzolan presence in the

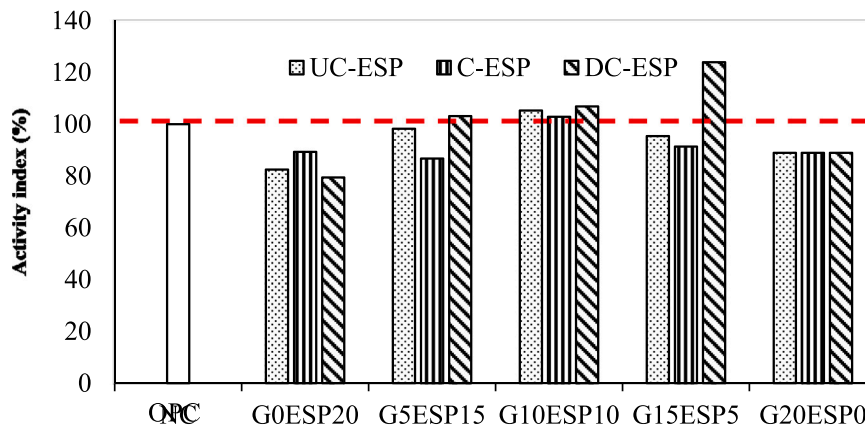


Fig. 27. Strength activity index for 7 days GPOFA-ESP mortar for UC-ESP, C-ESP and DC-ESP.

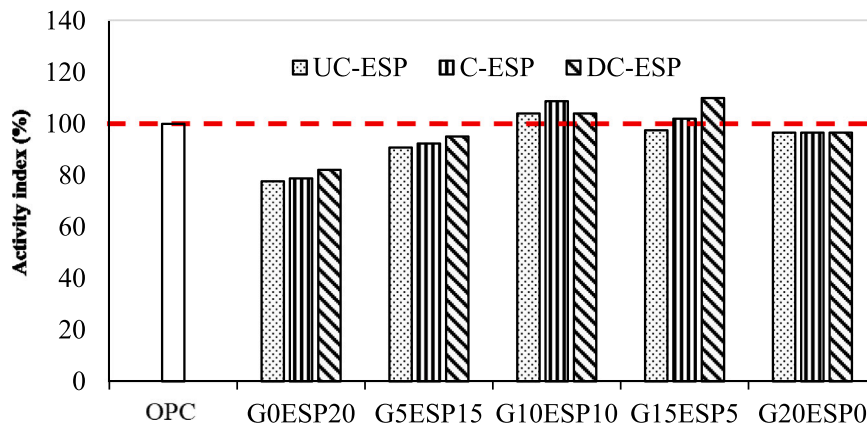


Fig. 28. Strength activity index for 28 days GPOFA-ESP mortar for UC-ESP, C-ESP and DC-ESP.

Table 7

Summary of strength activity index at 7 and 28 days.

Properties	Strength activity index (SAI)	
	7 days (%)	28 days (%)
OPC	-	-
GPOFA	89	97
Optimum G10UC10	105	104
Optimum G10C10	103	109
Optimum G5DC15	123	110
Permissible	≥ 75	≥ 75
Relevant standard	ASTM C311	ASTM C311

GPOFA concrete. The presence of CaO derived DC-ESP in water provides the formation of Ca(OH)₂; offer binary-reactivity of CaO. Both of the formations Ca(OH)₂ occurred which are the hydration product of reactivity in the concrete. When Ca(OH)₂ react with SiO₂ derived from GPOFA it was caused strength increased at the early age of the concrete.

4. Conclusions

This paper studied the transformation phase of eggshell powder (ESP) and their use with ground palm oil fuel ash (GPOFA) in cement concrete are examined. Based on the experimental test results the following conclusions are drawn:

- i. Three different phases of eggshell were successfully formed and prepared in this study by no heating (UC-ESP) and heating at 750 °C (C-ESP) and 1000 °C (C-ESP). The UC-ESP, C-ESP and C-

- ii. CaO derived DC-ESP showed better reactivity as compared to other two ESPs in cement concrete system. Mixed DC-ESP with GPOFA gave a superior CaO-SiO₂ reactivity in cement concrete, especially at the early age of strength development.
- iii. The highest compressive strength of the concretes was revealed; G10UC10, G10C10 and G15DC5 had superior compressive strength at both early and later age of concrete development. In addition, UC-ESP, C-ESP and DC-ESP had experienced as low, medium and superior accelerator behaviour in GPOFA concrete.
- iv. In overall, SiO₂-CaO had excellence synergy materials as accelerator in cement concrete by providing dual function; CaO and SiO₂ participate in the early and later ages of concrete strength development, respectively.
- v. The microstructure analysis (SEM) in term of strength shows good performance of GPOFA -ESPs concrete from an early age up to 90 days curing age.
- vi. In comparison to the OPC (control mortar) as a reference, the optimum GPOFA-ESP mixtures, i.e. G10UC10, G10C10 and G5DC15 mortar exhibited a higher SAI percentage of 105, 103 and 123 for 7 days curing time while 104, 109 and 110 for 28 curing age, respectively. On the other hand, the replacement with solely GPOFA exhibited SAI percentage of 89 for 7 days while 97 for 28 curing age. Based on the findings, it was observed that the strength activity indices at 7 and 28 days were exceeding the minimum permissible SAI of 75%. The SAI of G5DC15 mortar was

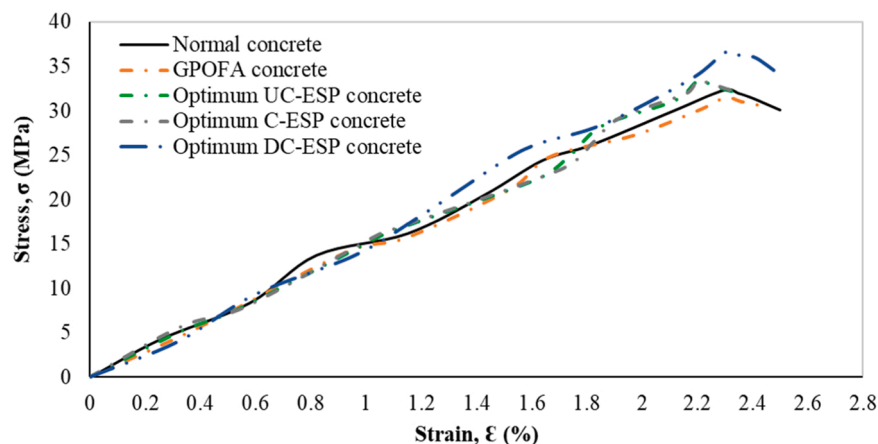


Fig. 29. Average stress-strain curves of normal concrete, GPOFA concrete, optimum UC-ESP concrete, optimum C-ESP concrete and DC-ESP concrete at 28 days of curing age.

seemed to be highest due to the acceleration effect of ESP as the early strength contributor while the decrement by GPOFA mortar was possibly attributed to the dilution effect which has delayed the pozzolanic reaction of GPOFA. The optimized GPOFA-ESP mixture sets have exhibited a higher SAI value due to the synergistic effect between ESP and GPOFA, which played their roles in early strength and later strength developer to improve the concrete performance.

5. Recommendations and future works

Based on the outcome of the research work, several recommendations for future study are highlighted as follow:

- i. The present study revealed that the incorporation of the GPOFA – ESPs produces concrete with excellent strength, therefore, it is also significant to expand the research investigation on the combination of high volume GPOFA and ESPs, and separation between early and later strength concrete.
- ii. It is also essential to study the effect of curing longer than 6 months on the carbonation of concrete containing GPOFA-ESPs concrete. This is an important study to ensure prolonged concrete performance with great strength and sustainability as a long-term concern.
- iii. Evaluate the effect of ESPs content on drying shrinkage and creep of proposed concrete.
- iv. The life cycle assessment (LCA) of GPOFA-ESPs should be investigated in the future study due to the significance of the study of green cementing materials development and its sustainability towards the environment.

CRedit authorship contribution statement

Majid Zaiton: Investigation, Formal analysis, Data curation. **Sam Abdul Rahman:** Validation, Supervision, Investigation. **Abd Khalid Nur Hafizah:** Writing – original draft, Formal analysis, Data curation, Conceptualization. **A. Rasid Nur Nadhira:** Writing – original draft, Resources, Investigation, Funding acquisition, Formal analysis, Data curation. **Huseien Ghasan:** Writing – review & editing, Software, Project administration. **Caronge Muhammad:** Validation, Project administration, Formal analysis. **Basar Norazah:** Visualization, Methodology, Conceptualization.

Declaration of Competing Interest

The authors whose names are listed immediately below certify that they have **NO** affiliations with or involvement in any organization or entity with any financial interest (such as honoraria; educational grants; participation in speakers' bureaus; membership, employment, consultancies, stock ownership, or other equity interest; and expert testimony or patent-licensing arrangements), or non-financial interest (such as personal or professional relationships, affiliations, knowledge or beliefs) in the subject matter or materials discussed in this manuscript. Author names:

Data Availability

Data will be made available on request.

Acknowledgement

The financial support for this project provided by the Universiti Teknologi Malaysia (UTM) and Ministry of High Education Malaysia (MoHE) under the grants of Q.J130000.3822.22H88, Q.J130000.2451.09G91, FRGS/1/2018/TK06/UTM/02/4 (R. J130000.7851.5F034), respectively.

References

- [1] A. Dowling, J.O. Dwyer, C.C. Adley, Lime in the limelight, *J. Clean. Prod.* 92 (2015) 3–22.
- [2] P. Faria, T. Santos, J. Aubert, Experimental characterization of an earth eco-efficient plastering mortar, *J. Mater. Civ. Eng.* 28 (1) (2016) 1–9.
- [3] M.R. Asgari, A.B. Dezfali, M. Bayat, Experimental study on stabilization of a low plasticity clayey soil with cement/lime, *Arab. J. Geosci.* 8 (2015) 1439–1452.
- [4] D.A. Emarah, S.A. Selem, Swelling soils treatment using lime and sea water for roads construction, *Alex. Eng. J.* 57 (4) (2018) 2357–2365.
- [5] V. Gitis, N. Hankins, Water treatment chemicals: Trends and challenges, *J. Water Process Eng.* 25 (2018) 34–38.
- [6] Z. Zhao, W. Li, F. Wang, Y. Zhang, Using of hydrated lime water as a novel degumming agent of silk and sericin recycling from wastewater, *J. Clean. Prod.* 172 (2018) 2090–2096.
- [7] A. Laca, A. Laca, M. Díaz, Eggshell waste as catalyst: A review, *J. Environ. Manag.* 197 (2017) 351–359.
- [8] S. Larsen, The Structure and Properties of Eggs, *Encycl. Food Chem.* 3 (2019) 27–32.
- [9] D. Cree, A. Rutter, Sustainable bio-Inspired limestone eggshell powder for potential industrialized applications, *ACS Sustain. Chem. Eng.* 3 (5) (2015) 941–949.
- [10] A.M. King'ori, A Review of the uses of poultry eggshells and shell membranes, *Int. J. Poult. Sci.* 10 (11) (2017) 908–912.
- [11] H.J. Park, S.W. Jeong, J.K. Yang, B.G. Kim, S.M. Lee, Removal of heavy metals using waste eggshell, *J. Environ. Sci.* 19 (12) (2007) 1436–1441.
- [12] R. Ahmad, R. Rohim, N. Ibrahim, Properties of waste eggshell as calcium oxide catalyst, *Appl. Mech. Mater.* 754–755 (2015) 171–175.
- [13] A. Arabhosseini, H. Faridi, Application of eggshell wastes as valuable and utilizable products: a review, *Res. Agric. Eng.* 64 (2) (2018) 104–114.
- [14] Veterinary Service Department, Livestock statistical 2017/2018 in Malaysia, 2018.
- [15] P. Pliya, D. Cree, Limestone derived eggshell powder as a replacement in Portland cement mortar, *Constr. Build. Mater.* 95 (2015) 1–9.
- [16] K.H. Mo, U.J. Alengaram, M.Z. Jumaat, S.C. Lee, W.I. Goh, C.W. Yuen, Recycling of seashell waste in concrete: a review, *Constr. Build. Mater.* 162 (2018) 751–764.
- [17] M. Balamurugan, R. Santhosh, Influence of eggshell ash on the properties of cement, *Imp. J. Interdiscip. Res.* 3 (4) (2017) 160–164.
- [18] K. Naemchanthara, S. Meejoo, W. Onreabroy, P. Limsuwan, Temperature effect on chicken eggshell investigated by XRD, TGA and FTIR, *Adv. Mater. Res.* 55–57 (2008) 333–336.
- [19] A.A. Jazie, H. Pramanik, A.S.K. Sinha, A.A. Jazie, Eggshell as eco-friendly catalyst for transesterification of rapeseed oil: optimization for biodiesel production, *Int. J. Sustain. Dev. Green. Econ.* 2 (2013) 27–32.
- [20] J. Goli, O. Sahu, Development of heterogeneous alkali catalyst from waste chicken eggshell for biodiesel production, *Renew. Energy* 128 (2018) 142–154.
- [21] A. Yerramala, Properties of concrete with eggshell powder as cement replacement, *Indian Concr. J.* 88 (10) (2014) 94–102.
- [22] M.O.A. Mtalib, A. Rabi, Effects of eggshells ash (ESA) on the setting time of cement, *Niger. J. Technol.* 28 (2) (2009) 29–38.
- [23] N. Shahadahtul, A. Asman, S. Dullah, J.L. Ayog, Mechanical properties of concrete using eggshell ash and rice husk ash as partial replacement of cement, *MATEC Web Conf.* 01002 (2017) 4–9.
- [24] K. Beck, X. Brunetaud, J.-D. Mertz, M. Al-Mukhtar, On the use of eggshell lime and tuffeau powder to formulate an appropriate mortar for restoration purposes, *Geol. Soc. Lond., Spec. Publ.* 331 (1) (2010) 137–145.
- [25] N.H.A. Khalid, M.W. Hussin, J. Mirza, N.F. Ariffin, M.A. Ismail, H. Lee, A. Mohamed, R.P. Jaya, Potential Effect of Palm Oil Fuel Ash as Micro-Filler of Polymer Concrete, *Constr. Build. Mater.* 102 (2015) 41–49.
- [26] ASTM C618–15, Standard specification for coal fly ash and raw or calcined natural pozzolan for use in concrete, West Conshohocken: ASTM International, 2015.
- [27] BS 8615–1:2019, Specification for pozzolanic materials for use with Portland cement. Natural pozzolana and natural calcined pozzolana, BSI Standards Publication, London, 2019.
- [28] J. Paya, M.V. Borrachero, J. Monzo, F. Amahjour, Enhanced conductivity measurement techniques for evaluation of fly ash pozzolanic activity, *Cem. Concr. Res.* 31 (2001) 41–49.
- [29] N.H. Roslan, M. Ismail, Z. Abdul-Majid, S. Ghoreishiamiri, B. Muhammad, Performance of steel slag and steel sludge in concrete, *Constr. Build. Mater.* 104 (2016) 16–24.
- [30] BS EN 12390–4:2000, Compressive strength- specification for testing machines: Part 4, BSI Standards Publication, London, 2000.
- [31] A.S.M.A. Awal, I.A. Shehu, Evaluation of heat of hydration of concrete containing high volume palm oil fuel ash, *Fuel* 105 (2013) 728–731.
- [32] N.H.A.S. Lim, M.A. Ismail, H.S. Lee, M.W. Hussin, A.R.M. Sam, M. Samadi, The effects of high volume nano palm oil fuel ash on microstructure properties and hydration temperature of mortar, *Constr. Build. Mater.* 93 (2015) 29–34.
- [33] BS EN 12390–3:2009, Compressive strength of test specimens: Part 3. BSI Standards Publication, London, 2011.
- [34] R.S. Boynton, Chemistry and technology of lime and limestone, 2nd edition, John Wiley & Sons, United States, 1980.
- [35] B. Engin, H. Demirtaş, M. Eken, Temperature effects on eggshells investigated by XRD, IR and ESR techniques, *Radiat. Phys. Chem.* 75 (2006) 268–277.
- [36] M. Mohammadi, P. Lahijani, A.R. Mohamed, Refractory dopant-incorporated CaO from waste eggshell as sustainable sorbent for CO₂ capture: Experimental and kinetic studies, *Chem. Eng. J.* 243 (2014) 455–464.
- [37] M. Galván-Ruiz, J. Hernández, L. Baños, J. Noriega-Montes, M.E. Rodríguez-García, Characterization of calcium carbonate, calcium oxide, and calcium

- hydroxide as starting point to the improvement of lime for their use in construction, *J. Mater. Civ. Eng.*, 21 (11) (2009) 694–698.
- [38] S. Gunasekaran, G. Anbalagan, S. Pandi, Raman and infrared spectra of carbonates of calcite structure, *J. Raman Spectrosc.* 37 (2006) 892–899.
- [39] R. Baxter, N. Hastings, A. Law, and E.J. Glass, *Understanding Cement*, 39 (5), WHD Microanalysis Consultatnts Ltd, 2008.